polysaccharides

MDPI

Article

Regenerated Cellulose Films from Vegetable Waste: Fabrication, Characterization, and Sustainable Applications

Adisak Jaturapiree, Ukrit Amphaiphan, Chanjira Jaramornburapong, Thanunya Saowapark, Kanjarat Sukrat and Ekrachan Chaichana *

Research Center of Natural Materials for Environment, Health and Beauty, Chemistry Program, Faculty of Science and Technology, Nakhon Pathom Rajabhat University, Nakhon Pathom 73000, Thailand; adisak@webmail.npru.ac.th (A.J.); ukrit@npru.ac.th (U.A.); chanjirajara@webmail.npru.ac.th (C.J.); thanunya@webmail.npru.ac.th (T.S.); kanjrat@npru.ac.th (K.S.)

* Correspondence: ekrachan@npru.ac.th

Abstract

Cellulose is a complex polysaccharide that serves as the primary structural component of plant cell walls. It is highly suitable for packaging films due to its inherent and tunable properties, which offer a sustainable alternative to conventional plastics. In this study, cellulose was extracted from vegetable waste (kale and cabbage) and processed into films using LiCl/N,N-dimethylacetamide (DMAc) as the solvent system. The regenerated cellulose films were characterized and compared with a film prepared from commercial microcrystalline cellulose (MCC) using the same procedure. The vegetable-waste films showed a lower degree of crystallinity than the MCC film. SEM micrographs revealed that the vegetable-waste films possessed smooth and uniform surfaces. Furthermore, they demonstrated good transparency, ductility, and thermal stability. Biodegradation tests indicated rapid decomposition of the vegetable-waste films, which fully degraded within 10 weeks, whereas the MCC film required 16 weeks. The cabbage-derived film exhibited a smoother surface and slightly better mechanical properties than the kale-derived film, suggesting that differences in the cellulose source can influence the regeneration process and, consequently, the properties of the resulting films. Overall, this work demonstrates that vegetable waste can be effectively upcycled into eco-friendly, low-cost cellulose films with strong potential for use in various sustainable material applications. Nevertheless, for edible applications, cytotoxicity testing is required to confirm the absence of residual health-risk reagents such as LiCl and DMAc in the resulting films.

Keywords: cellulose; waste management; regenerated film; biodegradable

Check for updates

Academic Editors: Lidija Fras Zemljič and Klementina Pušnik Črešnar

Received: 12 January 2026
Revised: 7 February 2026
Accepted: 6 May 2026
Published: 15 May 2026

Copyright: © 2026 by the authors. Licensee MDPI, Basel, Switzerland. This article is an open access article distributed under the terms and conditions of the Creative Commons Attribution (CC BY) license.

1. Introduction

The widespread use of petroleum-based plastics has resulted in severe environmental consequences, including long-term pollution, greenhouse gas emissions, and the accumulation of microplastics in terrestrial and aquatic ecosystems, posing health risks to all living organisms [1,2]. Consequently, the development of sustainable and eco-friendly alternatives has gained increasing attention across scientific and industrial sectors. Among these alternatives, natural polymers derived from biomass represent a promising class of materials due to their renewability, biodegradability, and low environmental footprint. Biomass resources such as agricultural residues, food waste, and lignocellulosic materials are abundantly available yet often underutilized, despite being rich in polysaccharides,

proteins, and other biopolymeric precursors. The valorization of these biomass sources not only contributes to waste reduction but also aligns with global initiatives toward a circular bioeconomy [3,4].

Cellulose, the most abundant renewable biopolymer on Earth, is primarily found in the cell walls of plants, agricultural waste, and wood. It offers great potential as a sustainable raw material for natural polymer development because of its biodegradability, structural versatility, and wide availability [5,6]. However, cellulose also presents certain limitations, particularly in processing. As a linear polymer composed of β (1→4)-linked D-glucose units, cellulose possesses a rigid and semi-crystalline structure stabilized by extensive hydrogen bonding. This results in its insolubility in water and most organic solvents, as well as difficulties in thermal processing. To overcome these challenges, numerous studies have explored the use of alternative solvent systems such as ionic liquids [7,8] deep eutectic solvents [9], NaOH/urea mixtures [10,11], and N-N-dimethylacetamide (DMAC)/LiCl systems [10,12] for dissolving cellulose and regenerating it into functional films. Among these, the DMAc/LiCl solvent system remains one of the most widely used and reliable for dissolving cellulose. In this system, chloride ions form strong hydrogen bonds with the hydroxyl groups on cellulose, effectively disrupting the intermolecular hydrogen-bonding network. Simultaneously, DMAc stabilizes the resulting complexes, allowing cellulose chains to disperse. As a result, DMAc/LiCl can dissolve even highly crystalline or high-molecular-weight cellulose without structural degradation, making it particularly valuable for both analytical applications and the fabrication of regenerated cellulose materials [5]. From an environmental perspective, both DMAc and LiCl exhibit relatively low toxicity, and the solvent system offers practical advantages such as low cost and high reusability compared with many emerging cellulose-dissolution platforms. Importantly, DMAc/LiCl can be recovered and reused multiple times with minimal reduction in performance, thereby decreasing solvent consumption, waste generation, and overall environmental impact [13]. Hence, these attributes position the DMAc/LiCl system as a powerful, efficient, and practical approach for cellulose dissolution, supporting the sustainable development of cellulose-based materials when managed responsibly.

Thailand is one of the world's major vegetable producers; however, a significant portion of these vegetables is discarded due to their short shelf life and imperfect appearance. Although still nutritionally suitable, such produce is often rejected by consumers, leading to substantial post-harvest losses and contributing to the growing volume of organic waste, especially in local markets and retail outlets. Most of this waste is either incinerated or sent to landfills, posing environmental challenges and representing a loss of valuable biomass [14]. Notably, many types of vegetable waste are rich in cellulose, a renewable biopolymer that can serve as a sustainable raw material for developing biodegradable materials. Given the increasing global demand for alternatives to petroleum-based plastics, the utilization of vegetable waste for producing regenerated cellulose films represents an environmentally friendly and economically viable solution.

Therefore, this study aims to investigate the feasibility of extracting cellulose from vegetable waste using the DMAc/LiCl solvent system and to evaluate its subsequent regeneration into biodegradable cellulose films. To the best of our knowledge, this is the first study to utilize vegetable waste as a primary raw material for producing regenerated cellulose films via solvent dissolution. This work explores the potential of these films for sustainable packaging and related applications, contributing to biomass valorization and advancing the principles of a circular bioeconomy.

2. Materials and Methods

2.1. Materials

Avicel, which is microcrystalline cellulose (MCC), and N-N-Dimethylacetamide (DMAC) of analytical grade were purchased from Sigma-Aldrich (Munich, Germany) Lithium chloride (LICl) extra pure, methanol 99.8%, and sodium hydroxide pellets 98% were purchased from Loba Chemie (Mumbai, India). Vegetable wastes were obtained from a local market in Nakornpathom province, Thailand.

2.2. Extraction and Purification of Cellulose

The objective of this study was to extract and purify cellulose from vegetable waste derived from cabbage (*Brassica oleracea*) and kale (*Brassica oleracea* var. sabellica). The vegetable wastes were cut and chopped into small pieces and then blended using a high-speed blender to obtain a fine pulp. The pulp was soaked in ethanol for 24 h to remove pigments and soluble impurities. Following this pretreatment, the pulp was boiled in 8% (*w*/*v*) sodium hydroxide (NaOH) solution for 2 h to eliminate non-cellulosic components such as lignin and hemicellulose. The resulting solid was washed repeatedly with deionized water until a neutral pH (∼7–8), measured using a pH meter (Mettler Toledo, Greifensee, Switzerland) was achieved. To further purify the cellulose, the residue was immersed in methanol under continuous stirring for 2 h and subsequently filtered under vacuum. The purified cellulose was dried in an oven at 105 °C for 4 h and stored in a desiccator until further use. The powder samples were designated as MCC_P for commercial cellulose powder (used as received) and Kal_P and Cab_P for cellulose powders obtained from kale waste and cabbage waste, respectively.

2.3. Preparation of Regenerated Cellulose Film

A cellulose sample (5 g), either cellulose powder extracted from vegetables (as described in the previous section) or commercial cellulose (Avicel) (5 g), was weighed and dispersed in 80 mL of N,N-dimethylacetamide (DMAC). The mixture was heated at 150 °C with continuous stirring for 30 min. Subsequently, 8 g of lithium chloride (LiCl) was added, and the solution was stirred for an additional 30 min under the same conditions. Afterward, the resulting cellulose solution was stirred at room temperature (30 °C) for 2–3 h to ensure complete dissolution and then centrifuged at 3000 rpm for 30 min to remove undissolved particles. The homogeneous solution was then cast onto a glass plate. The glass plate was gently immersed in deionized water for coagulation and fabrication. After that, the regenerated cellulose film was washed thoroughly with deionized water to remove all solvent and residue. Finally, the obtained cellulose film was dried in an oven at 60–65 °C for 24 h and stored in a desiccator until further use. The film samples were designated as MCC_F for films obtained from commercial cellulose powder and Kal_F and Cab_F for films obtained from kale waste and cabbage waste powders, respectively.

2.4. Characterization

The functional groups of the films were analyzed using Fourier-transform infrared (FTIR) spectroscopy. Spectra were recorded on a Thermo Scientific Nicolet iS5 FTIR spectrometer (Waltham, MA, USA) in transmittance mode over the wavenumber range of 400–4000 cm^{-1} with a resolution of 1 cm^{-1}.

The crystalline structure of the films was examined using X-ray diffraction (XRD) with a PANalytical Aeris diffractometer (Malvern Panalytical Ltd., Volketswil, The Netherlands). Measurements were performed using Cu Kα radiation (λ = 1.54 Å) over a 2θ range of 0–60° at a scan rate of 2° min^{-1}.

The mechanical properties of the films, including tensile strength and elongation at break, were determined according to ASTM D882-18 [15] using a Universal Testing Machine (UTM model NRI-TS-5S, Narin Instrument Company Limited, Samut Prakan, Thailand).

Color parameters (L*, a*, b*) were measured using a HunterLab UltraScan VIS benchtop spectrophotometer (HunterLab, VA, USA). The surface morphology of the films was investigated using scanning electron microscopy (SEM) (MIRA 3, Tescan, Brno–Kohoutovice, Czech Republic). Prior to imaging, samples were mounted on aluminum stubs and sputter-coated with gold for 15–30 s.

The thermal stability and decomposition behavior of the films were evaluated using thermogravimetric analysis (TGA) (Pyris I TGA, PerkinElmer, Inc., Waltham, MA, USA). Samples were heated from 30 to 800 °C at a constant heating rate of 30 °C min^{-1} under a nitrogen environment.

The water solubility of the films was determined according to the following procedure. The film samples were first dried in an oven at 110 °C until a constant weight (denoted as W_0) was obtained. Subsequently, the dried films were immersed in 50 mL of distilled water and stirred at 40 rpm using a magnetic stirrer at room temperature for hr. After immersion, the insoluble portions were separated by filtration and dried again in an oven until a constant weight (W_f) was reached. The water solubility (%) was calculated using the following equation:

$$\% \text{ water solubility} = \frac{W_0 - W_f}{W_0} \times 100 \quad (1)$$

The moisture content of the film was determined according to the following procedure. Film samples (2 cm × 2 cm) were dried at 105 °C until a constant weight was obtained (W_{dry}). The dried samples were then placed in a sealed desiccator containing a saturated sodium chloride (NaCl) solution to maintain a relative humidity (RH) of 75% for 24 h. After equilibration, the samples were weighed (W_{wet}). The moisture content was calculated using the following equation:

$$\% \text{ moisture } \frac{W_{wet} - W_{dry}}{W_{dry}} \times 100 \quad (2)$$

The water vapor permeation (WVP) of the film samples was determined according to a modified ASTM E96/E96M-24 [16] desiccant method. Each test cup was filled to approximately one-third of its volume with anhydrous calcium chloride ($CaCl_2$) to maintain a relative humidity (RH) of 0% inside the cup. Then, the cup was covered with the sample film slightly larger than the cup opening. The edges of the film were tightly sealed to prevent vapor leakage. The assembled cups were weighed to the nearest 0.001 g and then placed in a sealed desiccator containing a saturated sodium chloride (NaCl) solution, which provided an external RH of 75%. The cups were removed and weighed every 24 h using an analytical balance (±0.001 g). The weight gain of the cup was plotted against time, and the slope was determined by linear regression. The water vapor transmission rate (WVTR) was calculated as the slope divided by the area of the cup opening using the following equation:

$$WVP = \frac{WVTR \times X}{P(R2 - R1)} \quad (3)$$

where X is film thickness (mm^2). P is the saturated vapor pressure of water (Pa). R1 and R2 are the relative humidity (RH) inside and outside the cup. In this experiment, the driving force P(R2 − R1) was 1753.55 Pa.

2.5. Buried Test

Soil was placed into plastic foam boxes with internal dimensions of 32 × 39.5 × 14 cm^3. The film samples were cut into 2 × 2 cm^2 strips and buried at a depth of 4 cm beneath the soil surface. The boxes containing the soil and film specimens were incubated at ambient laboratory temperature (28–35 °C) while maintaining the soil moisture content at 20–40%. Each week, the buried film samples were carefully dug out and gently cleaned to remove adhering soil particles. The retrieved samples were then examined to evaluate changes in their physical appearance as an indicator of degradation.

3. Results and Discussion

3.1. Characterization of Regenerated Film

In this study, cellulose powders were first extracted from both vegetable wastes (cabbage and kale), along with a commercial cellulose powder (MCC). All cellulose powders were subsequently processed into regenerated cellulose films. The properties of both the powders and the films were further characterized to observe the differences among the samples and the changes induced by the film-forming process.

The crystalline structure of all samples was determined by X-ray diffraction (XRD) analysis. The XRD patterns of cellulose powders are compared with those of their corresponding cellulose films, as presented in Figure 1. All cellulose powder samples exhibit characteristic peaks of cellulose at 2θ ≈ 14.1°, 22.4°, and 34.5°, corresponding to the ($1\bar{1}0$), (200), and (004) planes, respectively. These reflections are indicative of a cellulose I crystalline structure [17]. However, the diffraction pattern of MCC powder shows a sharper peak at 22.4°, indicating higher crystallinity compared to the vegetable-derived powders. After dissolution and regeneration into films, the XRD patterns of all cellulose film samples shifted to higher 2θ values and exhibited lower intensity. This may be attributed to the disruption of hydrogen bonds between cellulose chains during dissolution, leading to a loss of crystallinity [18,19]. These changes suggest a transition toward a more amorphous cellulose structure. The MCC film still exhibits a characteristic cellulose peak of lower intensity, suggesting that it retains a slightly crystalline cellulose structure.

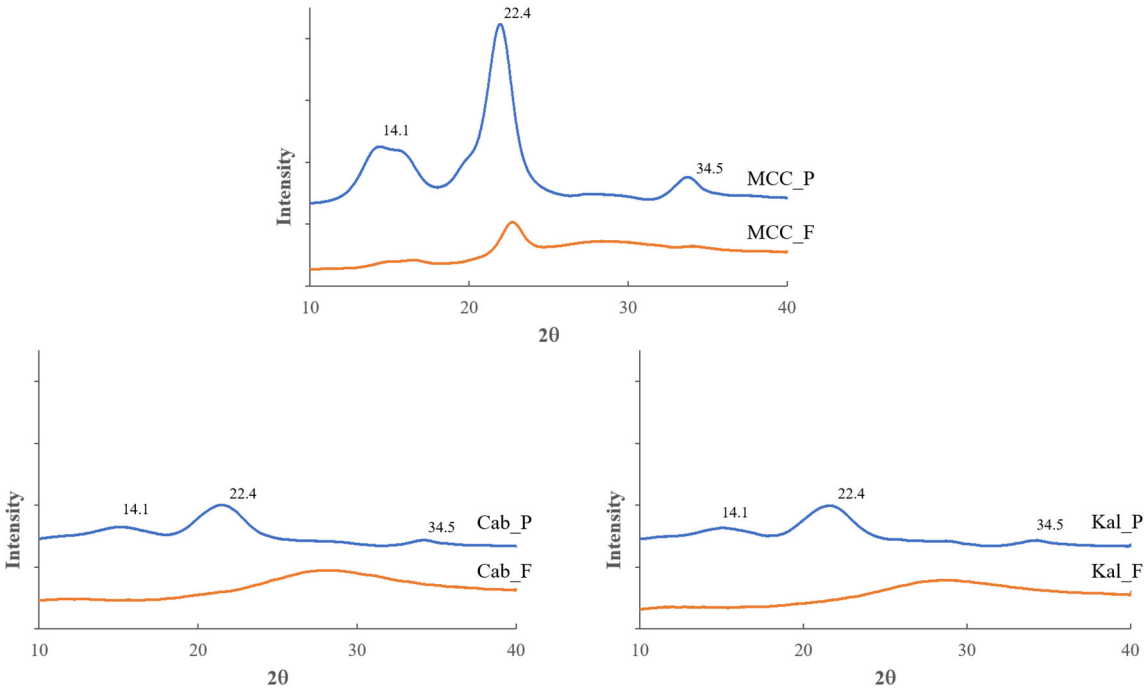


Figure 1. XRD patterns of regenerated cellulose powders and films.

When comparing the two vegetable-waste materials, the cellulose powder from cabbage (Cab_P) exhibits slightly higher crystallinity than that from kale (Kal_P), as evidenced by its more distinct diffraction peak at ~21–22° and a lower amorphous background. Nevertheless, in the corresponding films, Kal_F retains slightly higher crystallinity than Cab_F, as indicated by the more pronounced broad diffraction feature near 2θ ≈ 21–22°, whereas Cab_F shows a more amorphous diffraction profile. These results suggest that the crystallinity of regenerated films depends not only on the original structural order of the cellulose but also on other factors during the regeneration process. Variations in molecular weight distribution, chain flexibility, and hydrogen-bonding capability among celluloses from different vegetable sources significantly affect their dissolution behavior and subsequent film regeneration. Cellulose exhibiting a broader molecular weight distribution (MWD) and greater chain mobility tends to reorganize more efficiently during regeneration, promoting the formation of cellulose II-like or pseudo-crystalline domains, while more rigid, highly ordered chains preferentially form dense amorphous networks stabilized by strong hydrogen bonding [17,20,21]. The lower crystallinity of Kal_P may reflect a broader molecular weight distribution (MWD) than that of Cab_P, thereby contributing to the higher crystallinity of its regenerated film.

Fourier-transform infrared spectroscopy (FTIR) is a technique used to identify functional groups and to help suggest or confirm the presence of certain chemical substances. Accordingly, this technique was used to characterize the film samples to verify the presence of cellulose within their structures. The FTIR spectra of the samples are presented in Figure 2. All samples show similar characteristic peaks at 3336, 2898, 1633, 1420, 1371, 1155, 1020, and 895 cm^{-1}. These peaks correspond to the following vibrations: broad O–H stretching, C–H stretching in the cellulose backbone, H–O–H bending of absorbed water, CH_2 bending, C–H bending in the cellulose backbone, C–O–C symmetric stretching (β-1,4 linkage) in cellulose, C–O stretching of primary and secondary alcohol groups in glucose rings, and C–H deformation (β-glycosidic linkage) in the cellulose backbone, respectively. These spectral features are in good agreement with previously reported FTIR spectra of cellulose [22,23].

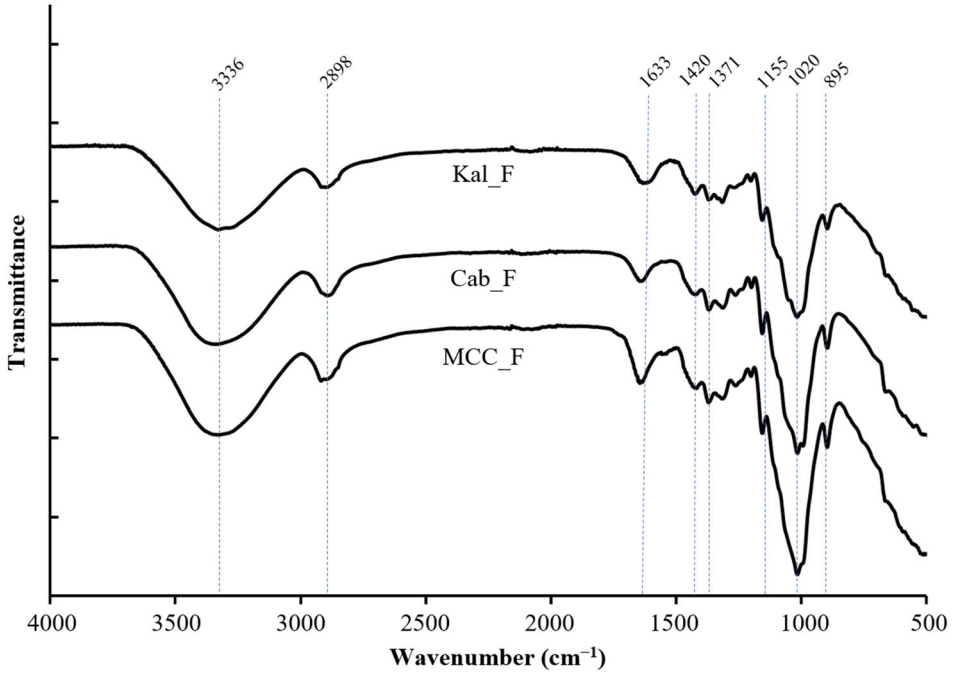


Figure 2. FTIR spectra of regenerated cellulose films.

No significant differences were observed among the FTIR spectra of the film samples, indicating the similarity of their cellulose functional groups. This suggests that the film-processing steps, including dissolution in the DMAc/LiCl solvent system, did not alter the functional groups of cellulose, which are critical in determining its chemical properties and reactivity.

The SEM images of the film samples are presented in Figure 3. All films exhibited slight surface wrinkling, which is likely associated with shrinkage during the regeneration step in water. Clear differences in surface morphology were observed when comparing the MCC film with the two vegetable-waste films. MCC_F exhibits a rough, highly fibrillated surface containing many microfibrils. In contrast, the films prepared from vegetable waste showed smooth and homogeneous surfaces, with only a few dispersed nanofibrillar features. This observation suggests that the DMAC/LiCl solvent system was effective in dissolving cellulose from vegetable waste. The improved solubility of vegetable-waste cellulose in DMAC/LiCl may be attributed to its comparatively more amorphous structure, which contains a higher degree of disorder and weaker intermolecular hydrogen bonding, as confirmed by the XRD pattern in Figure 1. Such structural characteristics likely facilitate solvent penetration and disruption of the polymer network, thereby enhancing dissolution efficiency [24]. The slightly higher surface roughness observed for Kal_F compared to Cab_F is likely associated with its higher crystallinity, especially under conditions of localized crystallization.

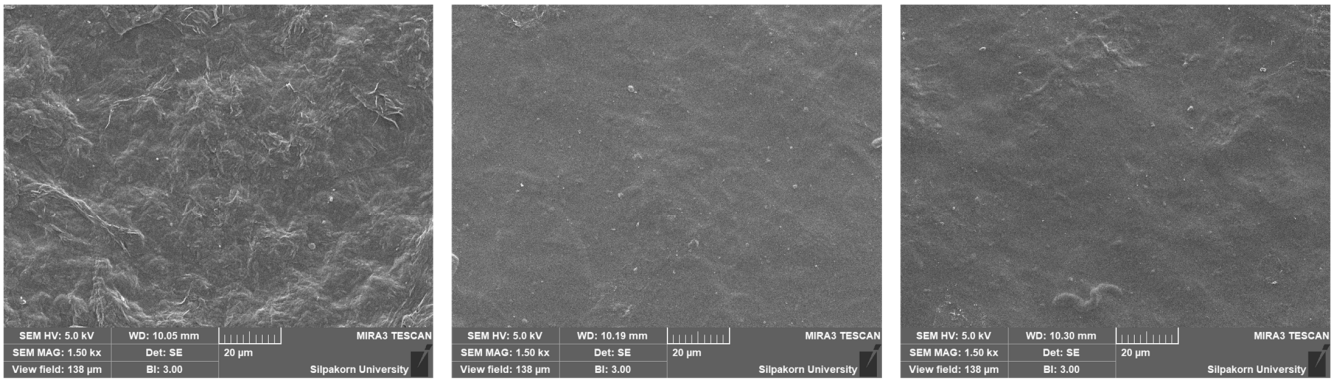


Figure 3. SEM images of regenerated cellulose films.

The UV–visible light transmittance spectra (200–800 nm) of the films with a thickness maintained at 10 ± 1 µm and the macroscopic images of all sample films are shown in Figures 4 and 5, respectively. Kal_F and Cab_F exhibited high transmittance values, reaching approximately 88% and 83% at 800 nm, respectively, which are significantly higher than that of the MCC film (53%). Kal_F and Cab_F exhibited higher transmittance than MCC_F across the entire wavelength range. At 800 nm, Kal_F and Cab_F reached transmittance values of approximately 88% and 83%, respectively, which are significantly higher than that of the MCC film (53%). These results are consistent with the macroscopic observations, wherein the kale and cabbage films appeared visually brighter and more transparent compared to the opaquer appearance of the MCC_F.

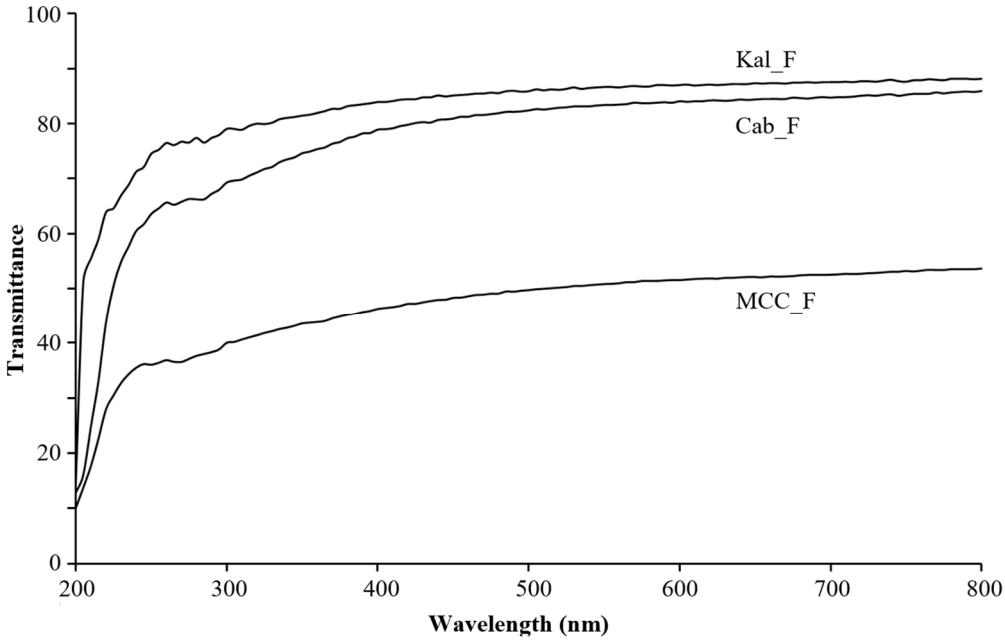


Figure 4. Transmittance spectra of regenerated cellulose films.



Figure 5. Macroscopic photograph of regenerated cellulose films.

The relatively low transmittance of MCC_F can be attributed to its high surface roughness and crystallinity. In contrast, the higher transmittance of Kal_F than Cab_F indicates that transparency is governed by multiple factors, including crystallite size and distribution, surface porosity, and film density, in addition to overall crystallinity and surface roughness.

LAB color measurement is a standardized analytical method based on the CIE L*a*b* color space, which comprises three coordinates: L*, representing lightness on a scale from 0 (black) to 100 (white); a*, indicating the chromatic position along the green–red axis (negative values denote green, positive values denote red); and b*, indicating the position along the blue–yellow axis (negative values correspond to blue, positive values to yellow). This color space enables precise quantification of color and is widely employed for evaluating the optical properties of films.

The LAB colorimetric data of film samples are presented in Table 1. It revealed that Kal_F exhibited the highest L* value (56.37), indicating the greatest lightness and the highest degree of translucency among the samples. In contrast, MCC_F recorded the lowest L* value (46.32), suggesting a more opaque and visually dense structure. Chromatically, MCC_F showed a moderately positive a* value (1.77), corresponding to a slight red undertone, while Kal_F (0.01) and Cab_F (−0.31) were closer to the neutral axis, with the latter exhibiting a minor green shift. Regarding the b* coordinate, MCC_F exhibited a high value (11.91), indicating a pronounced yellow hue, whereas Kal_F displayed a mild yellow tone (3.35). In

contrast, Cab_F showed a negative b* value (−1.11), suggesting a slight blue tint, which may be attributed to residual natural pigments in the vegetable wastes. These results quantitatively reflect the visual and chromatic differences observed among the films.

Table 1. Color value of regenerated cellulose films.

Sample	L*	a*	b*
MCC_F	40.37 ± 0.24	1.77 ± 0.14	11.91 ± 0.17
Kal_F	56.32 ± 0.15	0.01 ± 0.04	3.35 ± 0.09
Cab_F	50.28 ± 0.36	−0.31 ± 0.15	−1.11 ± 0.21

The contact angle is a fundamental parameter used to assess the surface wettability (hydrophilicity or hydrophobicity) of cellulose films. It represents the angle formed between the tangent of a water droplet and the solid surface. A larger contact angle indicates more hydrophobic behavior, where the liquid tends to bead up rather than spread on the surface. The contact angles of all regenerated films are presented in Figure 6. Among the samples, MCC_F exhibited the highest contact angle (74°), followed by Kal_F (50°) and Cab_F (48°). These results indicate that the MCC-F possesses a comparatively more hydrophobic surface than the films derived from vegetable waste. The higher contact angle observed for the MCC film can be attributed to its greater degree of crystallinity, as confirmed by the XRD analysis (Figure 1). This observation is consistent with previous reports [22,25], which demonstrated that cellulose films with higher crystallinity exhibit reduced wettability.

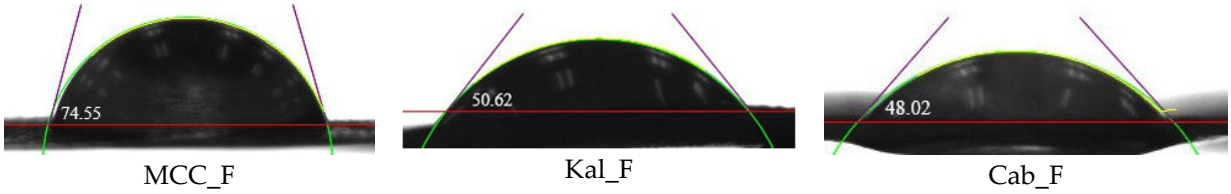


Figure 6. Contact angle of the regenerated cellulose films.

A higher crystallinity level corresponds to fewer accessible hydroxyl groups on the film surface, thereby decreasing the ability of water molecules to form hydrogen bonds with the cellulose chains. As a result, water droplets spread less readily across the surface, leading to an increased contact angle.

The water solubility, moisture content, and water vapor permeability (WVP) of the microcrystalline cellulose film (MCC_F), kale film (Kal_F), and cabbage film (Cab_F) are summarized in Table 2. Statistically significant differences ($p < 0.05$) were observed among the films for all evaluated parameters.

Table 2. Water solubility, moisture content, and water vapor permeability (WVP) of regenerated cellulose films.

Sample	Water Solubility (%)	Moisture (%)	WVP (10^{-7} g $h^{-1}m^{-1}Pa^{-1}$)
MCC_F	1.52 ± 0.49 ^{a}	9.86± 0.01 ^{a}	4.22 ± 0.55 ^{a}
Kal_F	5.83 ± 0.19 ^{b}	12.41 ± 0.37 ^{b}	7.33 ± 1.07 ^{b}
Cab_F	5.98 ± 0.36 ^{b}	12.60 ± 0.44 ^{b}	7.84 ± 0.74 ^{b}

Data are presented as mean ± standard deviation (SD) of three independent replicates. Different superscript letters within each column indicate statistically significant differences at $p < 0.05$.

MCC_F exhibited the lowest water solubility (1.52 ± 0.49%), whereas Kal_F and Cab_F showed significantly higher values of 5.83 ± 0.19% and 5.98 ± 0.36%, respectively. The

reduced solubility of MCC_F can be attributed to its higher crystallinity, as reported in the XRD pattern (MCC_F > Kal_F ≈ Cab_F). A higher crystalline fraction limits the accessibility of hydroxyl groups to water molecules, thereby restricting polymer–water interactions and reducing solubilization. In contrast, the kale- and cabbage-based films, with comparatively lower crystallinity and a higher amorphous content, allow easier penetration of water, resulting in increased solubility.

A similar trend was observed for moisture content, where MCC_F showed the lowest value (9.86 ± 0.01%), followed by Kal_F (12.41 ± 0.37%) and Cab_F (12.60 ± 0.44%). The higher moisture uptake in Kal_F and Cab_F is consistent with their more hydrophilic nature and lower molecular packing density. This observation aligns well with the contact angle measurements, where MCC_F displayed the highest contact angle, indicating a more hydrophobic surface, while Kal_F and Cab_F showed comparable and lower contact angles. The inverse relationship between contact angle and moisture content suggests that increased surface wettability promotes water absorption within the film matrix.

Water vapor permeability followed the same order, with MCC_F exhibiting the lowest WVP ($4.22 \pm 0.55 \times 10^{-7}$ g h^{-1} m^{-1} Pa^{-1}), significantly lower than Kal_F ($7.33 \pm 1.07 \times 10^{-7}$ g h^{-1} m^{-1} Pa^{-1}) and Cab_F ($7.84 \pm 0.74 \times 10^{-7}$ g h^{-1} m^{-1} Pa^{-1}). The superior water vapor barrier property of MCC_F can be explained by its higher crystallinity and compact microstructure, which create a more tortuous path for water vapor diffusion. In contrast, the more amorphous regions present in Kal_F and Cab_F facilitate water vapor transport, leading to increased permeability.

Overall, the combined effects of crystallinity, surface hydrophobicity, and polymer chain packing play a critical role in determining the water-related properties of the films. The strong correlation between lower crystallinity, reduced contact angle, and increased water solubility, moisture content, and WVP in Kal_F and Cab_F highlights the influence of vegetable-derived constituents on film performance. These findings suggest that while MCC_F offers superior moisture resistance and barrier properties, kale- and cabbage-based films may be more suitable for applications where higher water interaction or biodegradability is desired.

The mechanical performance of regenerated cellulose films is critical for their application in diverse fields. As illustrated in Figure 7, the tensile stress–strain behavior reveals that films regenerated from vegetable waste exhibit remarkable elongation at break, approximately 60% for Kal_F and 80% for Cab_F, compared to only 30% for MCC_F. However, the tensile strength of the vegetable waste-derived films is relatively lower. This can likely be attributed to their predominantly amorphous structure, in which cellulose chains are disordered and loosely packed. Such morphology leads to weaker intermolecular hydrogen bonding, increased free volume, and enhanced molecular mobility. Consequently, under applied tensile stress, the cellulose chains can undergo significant rearrangement and alignment, allowing the material to stretch extensively before failure [26,27].

Cab_F exhibits higher tensile strength and greater elongation at break than Kal_F. The larger elongation at break of Cab_F can be attributed to its more amorphous characteristics, as discussed earlier. The higher tensile strength may result from its higher molecular weight and the reduced formation of microvoids during film formation, as evidenced by its smoother surface.

Fracture surface analysis using SEM (Figure 8) revealed that tensile failure in all three film samples exhibited wave-like striations, indicating significant elongation prior to rupture. This feature was most prominently observed in films derived from vegetable waste. The initial thickness of the films was approximately 0.6–0.7 mm. After tensile testing to the point of failure, the thickness was reduced to 145.74, 61.62, and 52.74 μm for MCC_F,

Cab_F, and Kal_F, respectively. These results suggest that films derived from vegetable waste exhibit greater elongation capacity compared to those made from MCC.

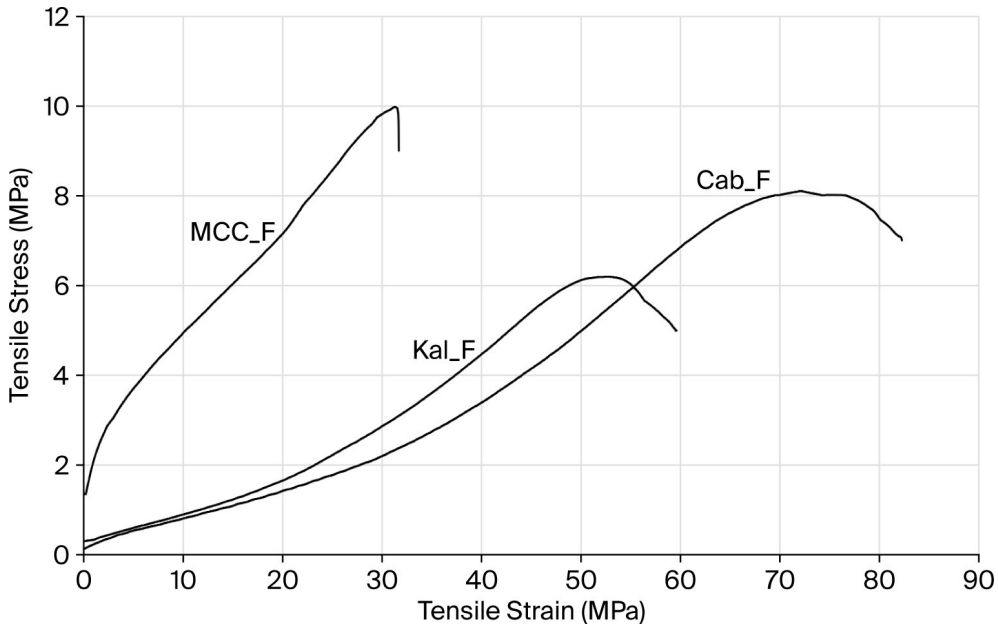


Figure 7. Stress–strain curves of regenerated cellulose films.

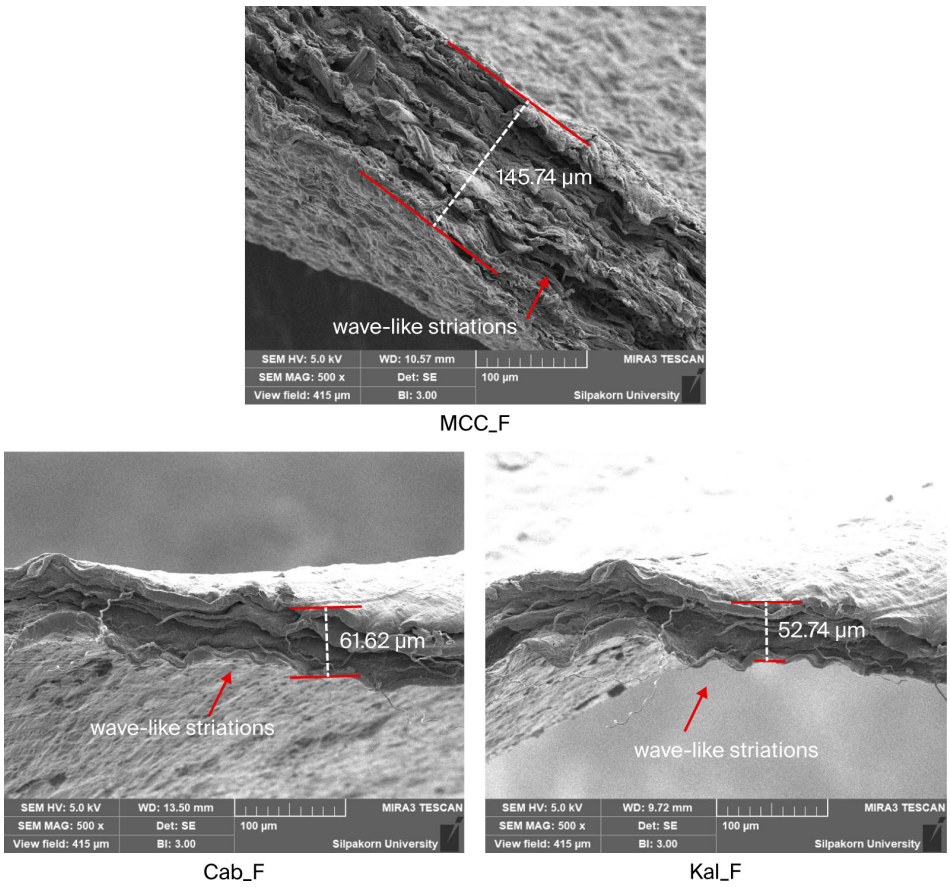


Figure 8. Fracture surface images of regenerated cellulose films after tensile testing.

Thermogravimetric analysis (TGA) and derivative thermogravimetric (DTG) analysis were employed to investigate the thermal stability and decomposition behavior of cellulose-

based films. As shown in Figure 9, all samples exhibited comparable thermal degradation profiles in both TGA and DTG curves. Two distinct stages of thermal degradation were observed. The first stage, occurring between approximately 100–150 °C, corresponds to the evaporation of physically adsorbed moisture. The second stage, occurring within the range of 250–400 °C, is attributed to cellulose breakdown. The onset of major degradation was found at 352.47 °C for MCC_F, 351.21 °C for Cab_F, and 347.85 °C for Kal_F. These values are consistent with previously reported data for regenerated cellulose films [28–30]. These results suggest that the thermal stability of cellulose films derived from vegetable waste is sufficiently high to support their potential use in various applications. The degradation temperatures were not found to correlate directly with film crystallinity based on the XRD results, indicating that other factors, including cellulose purity and residual species within the structure, play a more significant role in determining thermal stability.

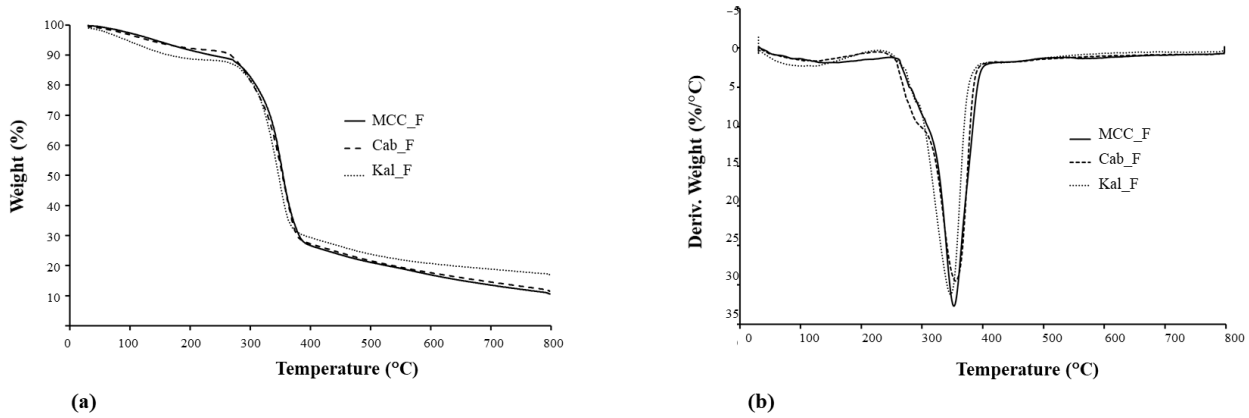


Figure 9. (**a**) TGA and (**b**) DTG curves of regenerated cellulose films.

3.2. Biodegradation Test

The biodegradation behavior of the cellulose films was evaluated by burying the samples in soil for twelve weeks. The biodegradation progress of the films is illustrated in Figure 10. After two weeks of soil exposure, both the vegetable-waste cellulose film and the microcrystalline cellulose film exhibited visible signs of degradation. The degradation of the vegetable-waste films (Cab_F and Kal_F) proceeded more rapidly, and by ten weeks, no residual fragments were detectable. In contrast, small remnants of MCC_F were still visible after 12 weeks. However, the complete degradation of MCC_F was observed within 16 weeks. No significant difference in biodegradation behavior was observed between the films prepared from kale and cabbage waste. Generally, an increase in the hydrophilicity of a polymer enhances microbial attachment and thereby accelerates biodegradation [31]. In addition, the crystallinity of the polymer is another crucial factor influencing degradation. Films with lower crystallinity are more susceptible to microbial attack in soil [32], leading to faster decomposition. Therefore, the faster biodegradation rate observed for the vegetable waste-derived cellulose films compared to the MCC film can be attributed to their higher hydrophilicity and lower crystallinity, as discussed in the earlier section. Although the obtained films exhibit good biodegradability, their direct application as edible films should be approached with caution, as some reagents used during film processing, such as LiCl and DMAc, pose potential health risks. Prior to any practical, commercial, or food-contact applications, comprehensive safety evaluations are strictly required.

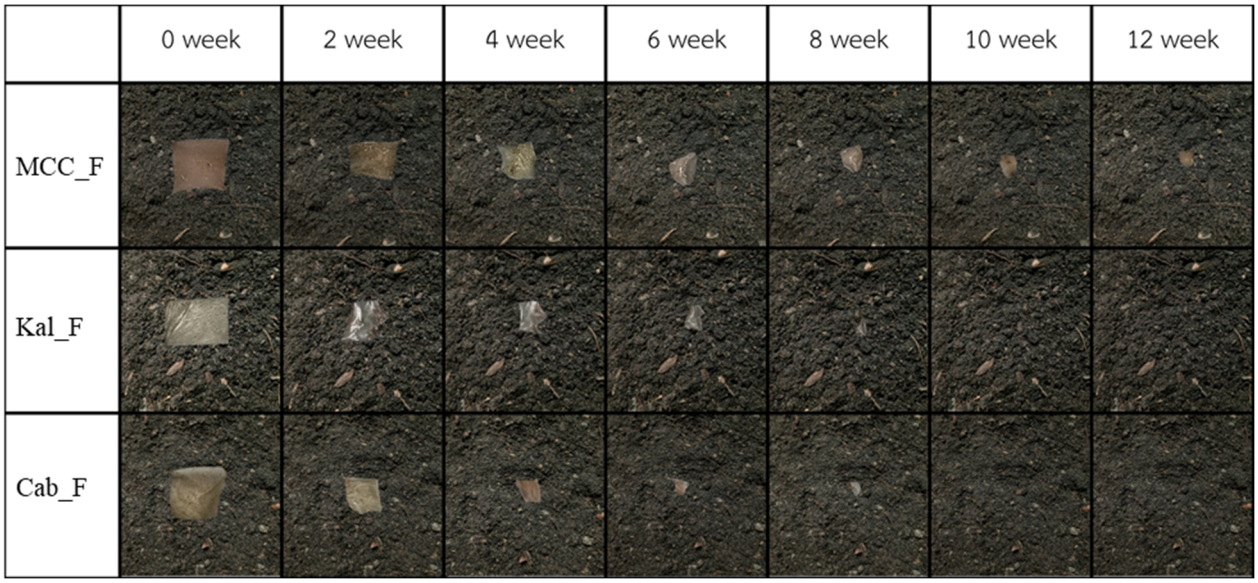


Figure 10. Digital photograph of regenerated cellulose films during soil burial tests.

4. Conclusions

In this experiment, regenerated cellulose films were produced from vegetable waste (kale and cabbage) and commercial microcrystalline cellulose using DMAC/LiCl as solvent. FTIR spectra and XRD patterns exhibited a change in the structure of the samples from crystalline cellulose to amorphous cellulose during the process. Compared with the MCC film, the films derived from vegetable waste exhibited greater transparency, ductility, hydrophilicity, and biodegradability, which can be attributed to their more amorphous structure. The cabbage-derived film exhibited a smoother surface and slightly better mechanical properties than the kale-derived film, suggesting that differences in the cellulose source influence the regeneration process and, consequently, the properties of the resulting films. Overall, these findings indicate that regenerated cellulose films derived from vegetable waste represent an eco-friendly and low-cost material. The films exhibit properties suitable for potential applications such as packaging, particularly for short-term or single-use purposes, where high biodegradability is required to reduce environmental impacts. For edible applications, cytotoxicity testing is required to confirm the absence of residual health-risk reagents such as LiCl and DMAc in the resulting films.

Author Contributions: Conceptualization, methodology, validation, and investigation, A.J., U.A. and C.J.; formal analysis and resources, A.J., U.A., C.J., K.S., T.S. and E.C.; writing—original draft preparation, A.J.; funding acquisition, U.A.; writing—review and editing, A.J. and E.C. All authors have read and agreed to the published version of the manuscript.

Funding: This research was funded by the National Research Council of Thailand, grant number TSRI_68_1.2.

Institutional Review Board Statement: Not applicable.

Data Availability Statement: The raw data supporting the conclusions of this article will be made available by the authors upon request.

Acknowledgments: The authors would like to thank the Research and Development Institute, Nakhon Pathom Rajabhat University, for research support.

Conflicts of Interest: The authors declare no conflicts of interest.

References

1. Sharma, S.; Sharma, V.; Chatterjee, S. Contribution of plastic and microplastic to global climate change and their conjoining impacts on the environment—A review. *Sci. Total Environ.* **2023**, *875*, 162627. [CrossRef] [PubMed]
2. Kumar, R.; Verma, A.; Shome, A.; Sinha, R.; Sinha, S.; Jha, P.K.; Kumar, R.; Kumar, P.; Shubham; Das, S.; et al. Impacts of Plastic Pollution on Ecosystem Services, Sustainable Development Goals, and Need to Focus on Circular Economy and Policy Interventions. *Sustainability* **2021**, *13*, 9963. [CrossRef]
3. Samuel, H.; Ekpan, F.-D.M.; Ori, M.O. Biodegradable, Recyclable, and Renewable Polymers as Alternatives to Traditional Petroleum-based Plastics. *Asian J. Environ. Res.* **2024**, *1*, 152–165. [CrossRef]
4. Ten, E.; Vermerris, W. Functionalized Polymers from Lignocellulosic Biomass: State of the Art. *Polymers* **2013**, *5*, 600–642. [CrossRef]
5. Acharya, S.; Liyanage, S.; Parajuli, P.; Rumi, S.S.; Shamshina, J.L.; Abidi, N. Utilization of Cellulose to Its Full Potential: A Review on Cellulose Dissolution, Regeneration, and Applications. *Polymers* **2021**, *13*, 4344. [CrossRef]
6. Isikgor, F.H.; Becer, C.R. Lignocellulosic biomass: A sustainable platform for the production of bio-based chemicals and polymers. *Polym. Chem.* **2015**, *6*, 4497–4559. [CrossRef]
7. Stojanović, D.; Ivanovska, A.; Barać, N.; Dimić-Misić, K.; Kostić, M.; Radojević, V.; Janaćković, D.; Uskoković, P.; Barceló, E.; Gane, P. Biodegradable Cellulose/Polycaprolactone/Keratin/Calcium Carbonate Mulch Films Prepared in Imidazolium-Based Ionic Liquid. *Polymers* **2023**, *15*, 2729. [CrossRef]
8. Zhao, J.; Ge, W.; Shuai, J.; Gao, X.; Zhang, F.; Wang, X. Efficient Cellulose Dissolution and Film Formation Enabled by Superbase Amino Acid Ionic Liquids. *Macromol. Rapid Commun.* **2023**, *44*, 2300175. [CrossRef]
9. Yu, J.; Liu, X.; Xu, S.; Shao, P.; Li, J.; Chen, Z.; Wang, X.; Lin, Y.; Renard, C.M.G.C. Advances in green solvents for production of polysaccharide-based packaging films: Insights of ionic liquids and deep eutectic solvents. *Compr. Rev. Food Sci.* **2023**, *22*, 1030–1057. [CrossRef] [PubMed]
10. Zhou, C.; Wang, Y. Recycling of waste cotton fabrics into regenerated cellulose films through three solvent systems: A comparison study. *J. Appl. Polym. Sci.* **2021**, *138*, 51255. [CrossRef]
11. Huang, K.; Maltais, A.; Liu, J.; Wang, Y. Wood cellulose films regenerated from NaOH/urea aqueous solution and treated by hot pressing for food packaging application. *Food Biosci.* **2022**, *50*, 102177. [CrossRef]
12. Sadeghifar, H.; Venditti, R.; Pawlak, J.; Jur, J. Cellulose transparent and flexible films prepared from DMAc/LiCl solutions. *Bioresources* **2019**, *14*, 9021–9032. [CrossRef]
13. Liu, J.; Zhang, H.; Jiang, X.; Tremblay, P.-L.; Zhang, T. An efficient and reusable N,N-dimethylacetamide/LiCl solvent system for the extraction of high-purity polyhydroxybutyrate from bacterial biomass. *Biochem. Eng. J.* **2023**, *192*, 108812. [CrossRef]
14. Ortiz-Gonzalo, D.; Ørtenblad, S.B.; Larsen, M.N.; Suebpongsang, P.; Bruun, T.B. Food loss and waste and the modernization of vegetable value chains in Thailand. *Resour. Conserv. Recycl.* **2021**, *174*, 105714. [CrossRef]
15. *ASTM D882-10*; Standard Test Method for Tensile Properties of Thin Plastic Sheeting. ASTM International: West Conshohocken, PA, USA, 2010.
16. *ASTM E96/E96M-24*; Standard Test Methods for Water Vapor Transmission of Materials. ASTM International: West Conshohocken, PA, USA, 2024.
17. French, A.D. Idealized powder diffraction patterns for cellulose polymorphs. *Cellulose* **2014**, *21*, 885–896. [CrossRef]
18. Zhang, X.; Xiao, N.; Wang, H.; Liu, C.; Pan, X. Preparation and Characterization of Regenerated Cellulose Film from a Solution in Lithium Bromide Molten Salt Hydrate. *Polymers* **2018**, *10*, 614. [CrossRef]
19. Lethesh, K.C.; Evjen, S.; Venkatraman, V.; Shah, S.N.; Fiksdahl, A. Highly efficient cellulose dissolution by alkaline ionic liquids. *Carbohydr. Polym.* **2020**, *229*, 115594. [CrossRef] [PubMed]
20. Klemm, D.; Heublein, B.; Fink, H.-P.; Bohn, A. Cellulose: Fascinating Biopolymer and Sustainable Raw Material. *Angew. Chem. Int. Ed.* **2005**, *44*, 3358–3393. [CrossRef] [PubMed]
21. Isogai, A.; Saito, T.; Fukuzumi, H. TEMPO-oxidized cellulose nanofibers. *Nanoscale* **2011**, *3*, 71–85. [CrossRef]
22. Pang, J.; Wu, M.; Zhang, Q.; Tan, X.; Xu, F.; Zhang, X.; Sun, R. Comparison of physical properties of regenerated cellulose films fabricated with different cellulose feedstocks in ionic liquid. *Carbohydr. Polym.* **2015**, *121*, 71–78. [CrossRef]
23. Huang, Z.; Liu, C.; Feng, X.; Wu, M.; Tang, Y.; Li, B. Effect of regeneration solvent on the characteristics of regenerated cellulose from lithium bromide trihydrate molten salt. *Cellulose* **2020**, *27*, 9243–9256. [CrossRef]
24. Ramos, L.A.; Assaf, J.M.; El Seoud, O.A.; Frollini, E. Influence of the Supramolecular Structure and Physicochemical Properties of Cellulose on Its Dissolution in a Lithium Chloride/N,N-Dimethylacetamide Solvent System. *Biomacromolecules* **2005**, *6*, 2638–2647. [CrossRef] [PubMed]
25. Yamane, C.; Aoyagi, T.; Ago, M.; Sato, K.; Okajima, K.; Takahashi, T. Two Different Surface Properties of Regenerated Cellulose due to Structural Anisotropy. *Polym. J.* **2006**, *38*, 819–826. [CrossRef]
26. Zhang, B.; Azuma, J.; Uyama, H. Preparation and characterization of a transparent amorphous cellulose film. *RSC Adv.* **2015**, *5*, 2900–2907. [CrossRef]

27. Kawano, T.; Iikubo, S.; Andou, Y. The Relationship between Crystal Structure and Mechanical Performance for Fabrication of Regenerated Cellulose Film through Coagulation Conditions. *Polymers* **2021**, *13*, 4450. [CrossRef]
28. Zhao, G.; Lyu, X.; Lee, J.; Cui, X.; Chen, W.-N. Biodegradable and transparent cellulose film prepared eco-friendly from durian rind for packaging application. *Food Packag. Shelf Life* **2019**, *21*, 100345. [CrossRef]
29. Reddy, K.O.; Maheswari, C.U.; Dhlamini, M.S.; Mothudi, B.M.; Zhang, J.; Zhang, J.; Nagarajan, R.; Rajulu, A.V. Preparation and characterization of regenerated cellulose films using borassus fruit fibers and an ionic liquid. *Carbohydr. Polym.* **2017**, *160*, 203–211. [CrossRef]
30. Knihs, A.F.; de Brito, B.B.; Granato, M.A.; Porto, B.; Siqueira Curto Valle, R.d.C.; Bierhalz, A.C.K. Cellulose regenerated films obtained from the dissolution of cotton waste in ionic liquid. *Colloid Polym. Sci.* **2024**, *302*, 2015–2026. [CrossRef]
31. Fiandra, E.F.; Shaw, L.; Starck, M.; McGurk, C.J.; Mahon, C.S. Designing biodegradable alternatives to commodity polymers. *Chem. Soc. Rev.* **2023**, *52*, 8085–8105. [CrossRef]
32. Ai, B.; Zheng, L.; Li, W.; Zheng, X.; Yang, Y.; Xiao, D.; Shi, J.; Sheng, Z. Biodegradable cellulose film prepared from banana pseudo-stem using an ionic liquid for mango preservation. *Front. Plant Sci.* **2021**, *12*, 625878. [CrossRef]

Disclaimer/Publisher's Note: The statements, opinions and data contained in all publications are solely those of the individual author(s) and contributor(s) and not of MDPI and/or the editor(s). MDPI and/or the editor(s) disclaim responsibility for any injury to people or property resulting from any ideas, methods, instructions or products referred to in the content.